Desalination and Water Treatment
www.deswater.com
doi: 10.5004/dwt.2023.29913

307 (2023) 171–179
September

Adsorption difference between Cu^{2+} and Zn^{2+} on sodium dodecyl sulfate/chitosan-modified semi-carbonized fibers

Wen-bin Li[a,†], Ru-yi Li[a,†], Hong-yan Deng[a,*], Li-na Wen[b,*], Bixia Wang[a], Abbas Touqeer[c], Hong Yang[d]

[a]*College of Environmental Science and Engineering, China West Normal University, Nanchong Sichuan 637009, China, emails: lwb062@163.com (W.-b. Li), dhongyan119@163.com (H.-y. Deng), 1551978946@qq.com (R.-y. Li), wangbixia@cwnu.edu.cn (B.-x. Wang)*
[b]*Sichuan Highway Planning, Survey, Design and Research Institute Ltd., Chengdu 610041, China, email: 26879619@qq.com (L.-n. Wen)*
[c]*Department of Soil, Water, and Climate, University of Minnesota, Twin 637009, USA, email: abbastouqeer@yahoo.com (A. Touqeer)*
[d]*Natural Forest Protection Project Management Center of Nanchong, Nanchong Sichuan 637009, China, email: 417823852@qq.com (H. Yang)*

Received 20 May 2023; Accepted 24 August 2023

ABSTRACT

Semi-carbonized polyacrylonitrile fiber (Spf) was modified with 50% and 100% sodium dodecyl sulfate (SDS) to prepare SDS-modified Spf (SDS-Spf) to explore the adsorption effect of heavy-metal ions on composite-modified fiber materials. Then, SDS-Spf was compositely modified with chitosan (CS) in different proportions (0%, 25%, 50%, and 100%) to obtain SDS and CS-modified Spf (SDS/CS-Spf). The isotherm adsorption characteristics of Cu^{2+} and Zn^{2+} on different SDS-Spfs and SDS/CS-Spfs were studied by batch method, and the effects of temperature, pH, and ionic strength on the adsorption were analyzed. The following results were obtained: (1) the adsorption isotherms of Cu^{2+} and Zn^{2+} on the tested samples all conformed to the Langmuir model, with the maximum adsorption capacity maintained at 1,007.60–1,156.03 (Cu^{2+}) and 856.08–970.50 mmol/kg (Zn^{2+}). They showed a trend of SDS/CS-Spf > SDS-Spf > Spf. (2) At 10°C–30°C, the adsorption amount of Cu^{2+} and Zn^{2+} on the tested materials increased with increasing temperature, and the adsorption exhibited a spontaneous, endothermic, and entropy-increasing process. (3) High pH facilitated the adsorption of Cu^{2+} and Zn^{2+} on the tested materials in the pH range of 2–6. With the increase in ionic strength, the adsorption amount of Cu^{2+} and Zn^{2+} increased first and then decreased, reaching the peak value at an ionic strength of 0.1 mol/L. (4) The pH, cation exchange capacity, and specific surface area of the different SDS/CS-Spfs determined the adsorption amount of Cu^{2+} and Zn^{2+}.

Keywords: Sodium dodecyl sulfate; Chitosan; Semi-carbonized fiber; Heavy metal; Adsorption amount

1. Introduction

With the rapid development of global economy, pollutants containing heavy metals enter soil through various channels, causing serious soil pollution [1]. Heavy-metal pollution in soil can affect the decline in crop yield and quality, harm human health through the food chain, and lead to further deterioration of water environmental quality [2]. Therefore, how to effectively control and treat soil

* Corresponding authors.
† These authors have contributed equally to this work and share first authorship.

heavy-metal pollution and improve soil quality are a hot and difficult research topics at present.

The basic principle of controlling and resolving heavy-metal pollution in soil is to remove or change the existing form of heavy metals in soil, thus reducing their mobility and bioavailability [3]. In accordance with the different types of heavy-metal pollution and soil types, the soil treatment measures and remediation methods for heavy-metal pollution can be divided into three categories: engineering physico-chemical methods, soil agrochemical regulation methods, and biological remediation methods [4]. Hou et al. [5] proposed that the treatment of heavy-metal pollution in soil by using soil improvement technology has fast effectiveness, thorough improvement, and high practicality. The leaching method mainly uses leaching agents to clean the soil, allowing pollutants in the soil to flow out with the leaching agent. Then, the leaching agent and the soil are subjected to subsequent treatment to achieve the goal of repairing the contaminated soil [6]. Zhu and Wei [7] used the filamentous prokaryote *Mycobacterium Hlei*, which has a high negative charge on the cell surface, to treat metal ions in the aqueous phase and achieved good results. Applying biochar can reduce soil acidity and the toxicity of toxic elements, such as aluminum and heavy metals, to plants [8]. The surface of biomass charcoal contains rich oxygen-containing functional groups, such as –COOH, –COOH, and –OH. The negative surface charges generated by these groups make the biomass charcoal have a high cation exchange capacity (CEC), which can improve the adsorption ability to heavy metals [9]. Biochar has strong adsorption capacity for heavy metals, and it can be used for remediation of contaminated soil [10,11]. Diatomaceous earth can fully convert exchangeable lead in soil into residual form [12].

Currently, the adsorption method in engineering physico-chemical methods for the remediation of heavy-metal-contaminated soil has become a mature technology and research hotspot. By adding adsorption materials to soil, the heavy-metal ions in it are fixed. The common adsorption materials include clay minerals, biochar, and nanomaterials [13–15]. Studies found that surface modification properties increased the adsorption performance of the material to heavy metals [16]. Yu et al. [17] found that ethylene diamine tetraacetic acid-modified bagasse can remarkably increase the adsorption capacity of Cu^{2+}, Cd^{2+}, and Pb^{2+}. The biosorbents obtained from saponification modification of fruit peel increased the number of carboxyl functional groups on their surface, their specific surface area (S_{BET}), and the internal porosity, showing good adsorption effect on Cu^{2+} in wastewater [18]. The adsorption performance of amphoteric-composite-modified clay minerals on heavy-metal ions in soil significantly improved [19].

Synthetic fiber is common in the decoration industry, and it has good flexibility. Carbonized fibers have large S_{BET} and good adsorption effect on heavy-metal ions. If the surface modification is carried out on carbonized fiber, its adsorption performance for heavy-metal ions can be greatly improved. However, few relevant reports are available. In the present study, sodium dodecyl sulfate (SDS) and chitosan (CS) were used to compositely modify semi-carbonized polyacrylonitrile fiber (Spf). The isotherm adsorption characteristics of Cu^{2+} and Zn^{2+} on different SDS and CS-modified Spfs were studied by batch method, and the effects of temperature, pH, and ionic strength on the adsorption were analyzed. The results could provide a theory basis for the technology of heavy-metal ion pollution by compound-modified materials.

2. Materials and methods

2.1. Experimental materials

SDS (analytic reagent, Tianjin Dingshengxin Chemical Co., Ltd., China) was used as anionic modifier. CS (analytic reagent, Shanghai Yuanye Biotechnology Co., Ltd., China) was used as composite modifier. Polyacrylonitrile fiber, obtained from Langfang City, Hebei Province, was used as the raw material. Solutions of heavy metal pollutants Cu^{2+} and Zn^{2+} were prepared using $CuSO_4{\cdot}5H_2O$ and $ZnSO_4$ (analytic reagent, Anhui Yuhuan Technology Co., Ltd., China), respectively. The structural formulas of SDS and CS are shown in Fig. 1.

2.1.1. Preparation of Spf

Polyacrylonitrile fiber was soaked in deionized water for 24 h and subsequently decolorized using ethanol. After decolorization, the raw material was placed in a muffle furnace at 300°C and stored in an anaerobic environment for 2 h. Following cooling, the material was ground through a 60-mesh screen to obtain Spf.

2.1.2. Preparation of SDS and CS-modified Spf (SDS/CS-Spf)

A certain weight of Spf was prepared for modification, slowly added to the prepared SDS solution with a Spf/water ratio of 1:10, and then dispersed by ultrasound at 60°C for 3 h. The samples were centrifuged at 4,800 rpm for 20 min, and the supernatant was separated. SDS-modified Spf (SDS-Spf) could be obtained after washing thrice with deionized water. SDS-Spf was dried at 60°C for 12 h and then passed through a 0.25-mm sieve. The compositely modification method was the same as the SDS modification, in which SDS-Spf was prepared for modification, and then CS was used to modify the SDS-Spf to obtain SDS and CS-modified Spf (SDS/CS-Spf). The dosage of SDS and CS were calculated using Eq. (1).

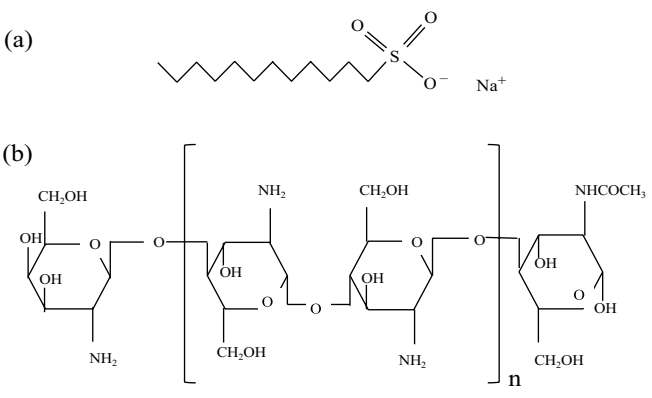

Fig. 1. Structural formulas of SDS (a) and CS (b).

$$W = m \times \mathrm{CEC} \times M \times 10^{-6} \times \frac{R}{b} \quad (1)$$

where W (g) is the quality of modifier. m (g) represents the mass of Spf or SDS-Spf. CEC (mmol/kg) denotes the CEC of Spf. M (g/mol) refers to the molecular mass of the modifier. R is the modified proportion. b stands for the content of the modifier product (mass fraction). The basic physical and chemical properties of the tested samples are shown in Table 1.

2.2. Experimental design

2.2.1. Isothermal adsorption experiment

Spf was modified by 50% and 100% SDS to obtain 50SDS-Spf and 100SDS-Spf, then 50SDS-Spf and 100SDS-Spf were secondly modified by 25%, 50%, and 100% CS to prepare 50SDS/25CS-Spf, 50SDS/50CS-Spf, 50SDS/100CS-Spf, 100SDS/25CS-Spf, 100SDS/50CS-Spf, and 100SDS/100CS-Spf. With Spf as the control, a total of 9 samples were subjected to adsorption isotherm experiments. The experimental temperature is set to 30°C, the pH value is set to 6, and 0.1 mol/L NaCl solution is used as the background ionic strength.

2.2.2. Influence of environmental factors

The experimental temperatures were set at 10°C, 20°C, and 30°C; the pH of the solution was set at 6; and the ionic strength was set at 0.1 mol/L NaCl. The initial pH values of the solution were set as 2, 4, and 6; the solution temperature was set as 30°C; and the ionic strength was set as 0.1 mol/L NaCl. The initial ionic strength of the solution was set to 0.05, 0.1, and 0.2 mol/L NaCl; the solution temperature was set to 30°C; and the pH value was set to 6.

2.3. Experiment method

Batch equilibrium method was used for Cu^{2+} and Zn^{2+} adsorption. A total of 0.1000 g of the sample was weighed in nine 50 mL plastic centrifuge tubes and added with 20 mL of Cu^{2+} and Zn^{2+} solutions with different concentration gradients. The samples were oscillated at 20°C and 200 rpm for 12 h at constant temperature and centrifuged at 4,800 rpm for 10 min. The concentration of Cu^{2+} and Zn^{2+} in the supernatant was determined, and the equilibrium adsorption amount was calculated by subtraction method. Cu^{2+} and Zn^{2+} was measured using the Hitachi Z-5000 atomic absorption spectrophotometer using flame method, with Zeeman effect correction for background absorption. All the above measurements were inserted into the standard solution for analysis quality control.

Table 1
Basic physical and chemical properties of the tested materials

Tested materials	pH	CEC (mmol/kg)	S_{BET} (m^2/g)
Spf	8.01	87.25	1.38
50SDS-Spf	7.64	93.35	1.87
50SDS/25CS-Spf	7.54	88.56	1.97
50SDS/50CS-Spf	7.47	90.13	1.99
50SDS/100CS-Spf	7.34	100.45	2.03
100SDS-Spf	7.23	154.33	1.94
100SDS/25CS-Spf	7.22	134.22	2.03
100SDS/50CS-Spf	7.14	140.24	2.12
100SDS/100CS-Spf	7.05	166.34	2.16

2.4. Data processing

2.4.1. Equilibrium adsorption amount

The equilibrium adsorption amount was calculated using Eq. (2):

$$q = \frac{V \times \left(C_0 - C_1\right)}{W_0} \quad (2)$$

where C_0 (mmol/L) and C_1 (mmol/L) are the initial and equilibrium concentrations of Cu^{2+} (or Zn^{2+}) in the solution, respectively. V (mL) is the volume of Cu^{2+} (or Zn^{2+}) solution added. W_0 (g) is the weight of the tested soil sample. q (mmol/kg) is the equilibrium adsorption amount of Cu^{2+} (or Zn^{2+}) on the tested soil.

2.4.2. Fitting of adsorption isotherms

The Langmuir isotherm was selected on the basis of the adsorption isotherm trend and the isothermal equation [Eq. (3)] is as follows [20]:

$$q = \frac{q_m b C_1}{1 + bC_1} \quad (3)$$

where q_m indicates the maximum adsorption amount of Cu^{2+} (or Zn^{2+}) on the different materials, mmol/kg; b represents the apparent equilibrium constant of the Cu^{2+} (or Zn^{2+}) adsorption, which can be used to measure the affinity of adsorption.

2.4.3. Calculation of thermodynamic parameters

Parameter b in the Langmuir model is equivalent to the apparent adsorption constant of equilibrium constant, and the thermodynamic parameter calculated by $b = K$ is called the apparent thermodynamic parameters, Eqs. (4)–(6) [21]:

$$\Delta G = -RT \ln K \quad (4)$$

$$\Delta H = R\left(\frac{T_1 \cdot T_2}{T_2 - T_1}\right) \cdot \ln\left(\frac{K, T_2}{K, T_1}\right) \quad (5)$$

$$\Delta S = \frac{\Delta H - \Delta G}{T} \quad (6)$$

where ΔG is the standard free energy change (kJ/mol), R is a constant (8.3145 J/mol·K), T is the adsorption temperature (T_1 = 283.16 K and T_2 = 303.6 K), ΔH is the enthalpy of adsorption process (kJ/mol), and ΔS is the entropy change of adsorption process (J/mol·K).

CurveExpert 1.4 fitting software was used in isothermal fitting, and Origin 9.0 software was adopted to improve data plotting. The data were expressed as the means with standard deviation, and different letters indicate significant differences among various amendments. Analysis of variance was performed to determine the effects of amendments, followed by Tukey's honestly significant difference test. Differences of $P < 0.05$ were considered significant.

3. Results and discussion

3.1. Isothermal adsorption characteristics of Cu^{2+} and Zn^{2+}

The adsorption isotherms of Cu^{2+} and Zn^{2+} on different modified Spfs are shown in Fig. 2. The adsorption capacity of different modified Spfs for Cu^{2+} and Zn^{2+} increased with the increase in equilibrium concentration, showing L-shaped adsorption curves. At the same equilibrium concentration, the adsorption capacity of SDS/CS-Spf was higher than that of SDS-Spf. The Langmuir model was used to fit the adsorption isotherm of Cu^{2+} and Zn^{2+} by different modified Spfs (Table 2). The correlation reached a very significant level ($P < 0.01$). Thus, the adsorption of Cu^{2+} and Zn^{2+} by the modified Spfs suited the description by the Langmuir adsorption model.

The maximum adsorption capacity (q_m) values of Cu^{2+} and Zn^{2+} on each modified Spf were 1,007.60–1,156.03 and 856.08–970.50 mmol/kg, respectively. The q_m of Cu^{2+} and Zn^{2+} showed a trend of 100SDS/100CS-Spf > 100SDS/50CS-Spf > 50SDS/100CS-Spf > 100SDS/25CS-Spf > 50SDS/50CS-Spf > 50SDS/25CS-Spf > 100SDS-Spf > 50SDS-Spf > Spf, which is consistent with the trend of adsorption isotherms in Fig. 2. With the increase in the modification proportion of SDS and CS, the adsorption amount of Cu^{2+} and Zn^{2+} increased. The q_m of Cu^{2+} and Zn^{2+} on SDS-Spfs and SDS/CS-Spfs were 16.33–106.42 mmol/kg higher than that on Spf. The above results indicated that SDS and CS modifications increased the adsorption capacity of Spf for heavy metals, consistent with the result of previous studies on Cd^{2+} adsorption onto CS+SDS-modified bentonite [22].

3.2. Effect of temperature on Cu^{2+} and Zn^{2+} adsorption

Within the range of 10°C–30°C, the adsorption changes in Cu^{2+} and Zn^{2+} on each modified Spf are shown in Fig. 3. With the increase in temperature, the adsorption amount of Cu^{2+} and Zn^{2+} on the test materials increased, showing a positive temperature effect. When the temperature was changed from 10°C to 30°C, the adsorption amounts of Cu^{2+} and Zn^{2+} on different modified Spfs increased by 27.65–77.93 and 82.56–193.65 mmol/kg, respectively. These results are mainly related to the chemisorption of Cu^{2+} and Zn^{2+} of the different modified Spfs, and the increase in temperature can intensify the irregular thermal movement of Cu^{2+} and Zn^{2+}. Such intensification is conducive to the full contact of Cu^{2+} and Zn^{2+} with the adsorption sites of the improved materials to enhance the adsorption effect. The intensification is also the result of the combined action of ion exchange, charge attraction, and surface complexation, confirming that the above adsorption process is a chemical endothermic reaction [23].

Table 3 shows the thermodynamic parameters of the adsorption of Cu^{2+} and Zn^{2+} on the modified Spfs. At 10°C

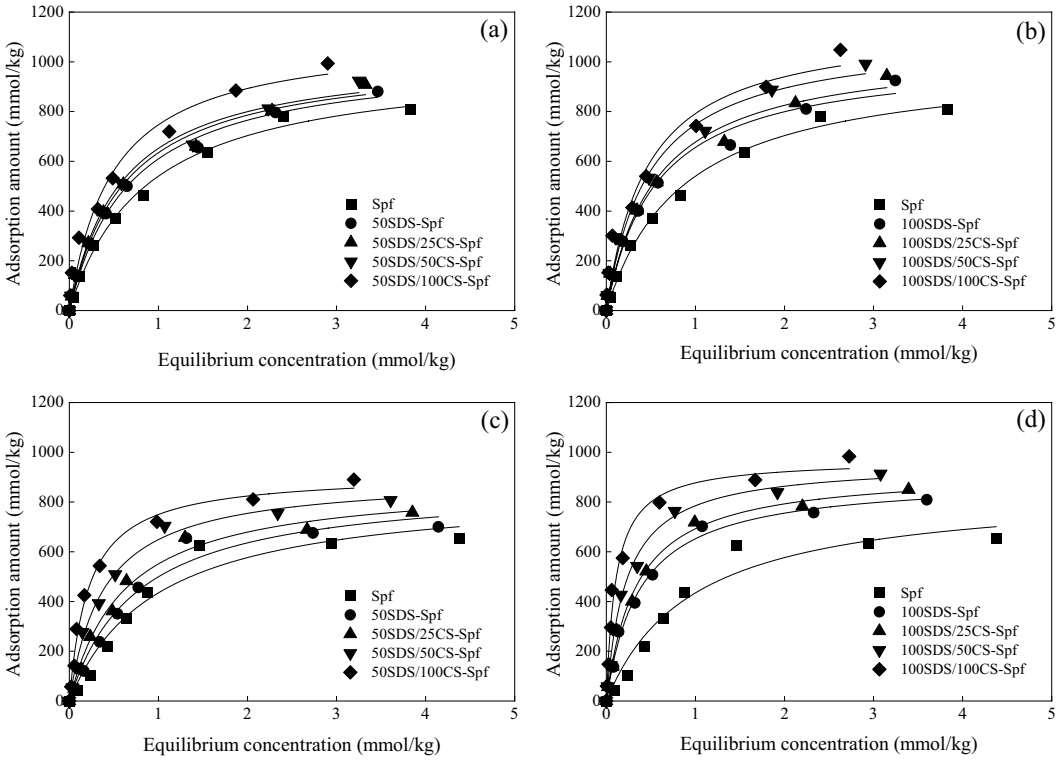

Fig. 2. Adsorption isotherm of Cu^{2+} (a and b) and Zn^{2+} (c and d) on the tested materials.

Table 2
Fitting parameters of Cu^{2+} and Zn^{2+} adsorption isotherm

Tested samples		q_m (mmol/kg)	b	Standard deviation (S)	Correlation coefficient (r)
	Spf	1,007.60	1.16	565.18	0.9939**
	50SDS-Spf	1,023.93	1.46	499.94	0.9952**
	50SDS/25CS-Spf	1,031.06	1.60	1,051.96	0.9902**
	50SDS/50CS-Spf	1,034.01	1.71	1,607.87	0.9854**
C^{u2}+	50SDS/100CS-Spf	1,109.81	2.06	3,521.92	0.9727**
	100SDS-Spf	1,026.59	1.78	1,603.61	0.9854**
	100SDS/25CS-Spf	1,055.15	1.79	1,974.38	0.9829**
	100SDS/50CS-Spf	1,111.08	2.06	3,288.48	0.9746**
	100SDS/100CS-Spf	1,156.03	2.17	6,492.85	0.9535**
	Spf	856.08	1.03	3,177.90	0.9536**
	50SDS-Spf	875.13	1.33	2,152.51	0.9719**
	50SDS/25CS-Spf	884.28	1.65	1,139.39	0.9862**
	50SDS/50CS-Spf	901.09	2.57	612.34	0.9936**
Zn^{2+}	50SDS/100CS-Spf	926.63	4.55	1,039.64	0.9906**
	100SDS-Spf	896.84	2.67	614.58	0.9935**
	100SDS/25CS-Spf	914.22	2.96	639.53	0.9938**
	100SDS/50CS-Spf	959.24	4.50	954.74	0.9920**
	100SDS/100CS-Spf	970.50	9.39	2,270.38	0.9832**

Note: ** indicates significance at the $p = 0.01$ level ($r = 0.765$ at $p = 0.01$ when the degrees of freedom $f = 8$).

Table 3
Adsorption thermodynamic characteristic CS of Cu^{2+} and Zn^{2+}

Tested samples	Cu^{2+}				Zn^{2+}			
	ΔG (kJ/mol)		ΔH (kJ/mol)	ΔS (J/mol·K)	ΔG (kJ/mol)		ΔH (kJ/mol)	ΔS (J/mol·K)
	10°C	30°C			10°C	30°C		
Spf	–16.50	–17.77	5.50	77.68	–15.91	–17.49	6.98	80.83
50SDS-Spf	–17.08	–18.37	5.35	79.24	–16.63	–18.13	6.33	81.10
50SDS/25CS-Spf	–17.24	–18.60	5.58	80.59	–16.99	–18.68	6.98	84.67
50SDS/50CS-Spf	–17.41	–18.76	5.48	80.85	–18.01	–19.79	6.94	88.13
50SDS/100CS-Spf	–17.77	–19.23	5.82	83.32	–19.30	–21.23	7.03	92.98
100SDS-Spf	–17.51	–18.87	5.48	81.22	–18.10	–19.88	6.94	88.42
100SDS/25CS-Spf	–17.55	–18.88	5.40	81.03	–18.32	–20.15	7.02	89.50
100SDS/50CS-Spf	–17.80	–19.23	5.69	82.96	–19.24	–21.20	7.15	93.21
100SDS/100CS-Spf	–17.94	–19.37	5.64	83.28	–21.10	–23.05	6.53	97.58

and 30°C, the Gibbs free energy variation (ΔG) of Cu^{2+} and Zn^{2+} adsorption on each test material was less than 0, indicating that the adsorption process of Cu^{2+} and Zn^{2+} was spontaneous, and the spontaneity at 30°C was stronger than at 10°C under the same material. The enthalpy change (ΔH) of the modified Spfs were greater than zero, indicating that the adsorption was an endothermic reaction. The increase in temperature can increase the thermal process of Cu^{2+} and Zn^{2+} and promote the chemisorption process. This result mutually supported the conclusion that increasing temperature is beneficial to the adsorption of Cu^{2+} and Zn^{2+} (Fig. 3). The entropy change (ΔS) of the modified Spfs were all greater than zero, indicating that the adsorption belonged to entropy-increasing reaction. Hence, the randomness of Cu^{2+} and Zn^{2+} at the solid–liquid interface increased during the adsorption process [24].

3.3. Effect of pH on Cu^{2+} and Zn^{2+} adsorption

Comparison among the adsorption changes of Cu^{2+} and Zn^{2+} on the modified Spfs under different pH levels showed that the adsorption amount of Cu^{2+} and Zn^{2+} had the same trend (Fig. 4). In the pH range of 2–6, the adsorption amount of Cu^{2+} and Zn^{2+} on the modified Spfs increased with the increase in pH and presented the largest at pH = 6. This result showed that the change in pH had a substantial effect on the adsorption of Cu^{2+} and Zn^{2+} on the modified Spfs. At low pH conditions, a competitive adsorption between

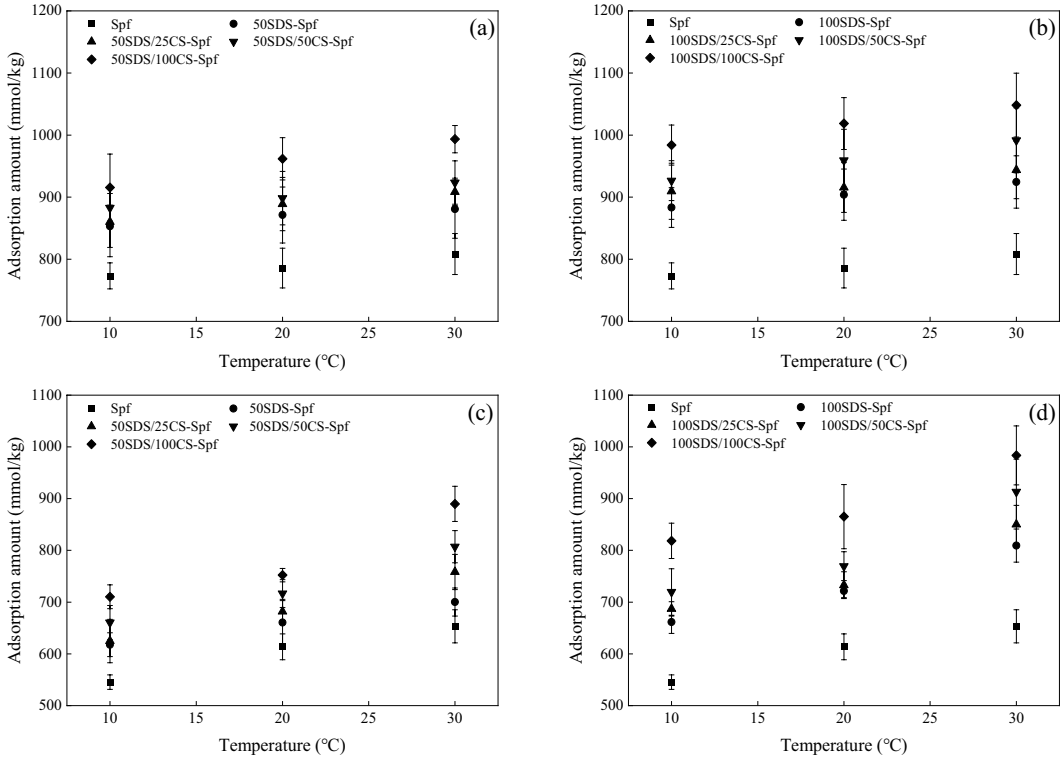

Fig. 3. Effect of temperature on the adsorption of Cu^{2+} (a and b) and Zn^{2+} (c and d).

Table 4
Relationship between adsorption parameters and physico-chemical properties of the tested materials

Adsorption parameters		Physico-chemical properties	Regression equation	*r*	*S*
Cu^{2+}	q_m	pH	$pH = -0.0043q_m + 11.95$	0.7369*	0.22
		CEC	$CEC = 0.3669q_m - 272.36$	0.5975	26.96
		S_{BET}	$S_{BET} = 0.0031q_m - 1.30$	0.6829*	0.18
	b	pH	$pH = -0.8607b + 8.91$	0.9297**	0.12
		CEC	$CEC = 65.7005b + 1.94$	0.6717*	24.91
		S_{BET}	$S_{BET} = 0.6332b + 0.83$	0.8899**	0.11
Zn^{2+}	q_m	pH	$pH = -0.0069q_m + 13.70$	0.8777**	0.15
		CEC	$CEC = 0.5990q_m - 427.51$	0.7194*	23.35
		S_{BET}	$S_{BET} = 0.0049q_m - 2.48$	0.8026**	0.15
	b	pH	$pH = -0.0851b + 7.69$	0.7345*	0.216
		CEC	$CEC = 8.6902b + 87.61$	0.7098*	23.68
		S_{BET}	$S_{BET} = 0.0560b + 1.75$	0.6290	0.19

Note: ** and * respectively indicate significant correlation at the level of $P = 0.01$ and $P = 0.05$.

H^+ occurred. With the increase in pH, the number of OH^- ions increased, which easily coprecipitated with Cu^{2+} and Zn^{2+}, and the competitive adsorption weakened [25].

3.4. Effect of ionic strength on Cu^{2+} and Zn^{2+} adsorption

When the ionic strength changed from 0.05 to 0.20 mol/L, the adsorption amount of Cu^{2+} and Zn^{2+} on all the modified Spfs increased first and then decreased (Fig. 5). When the ionic strength increased from 0.05 to 0.2 mol/L, the adsorption amounts of Cu^{2+} and Zn^{2+} on the modified Spfs decreased by 1.01–16.59 and 18.35–59.11 mmol/kg, respectively. These results were mainly due to the low electrolyte content at low ionic strength. With the increase in ionic strength of the solution, the conductivity of the solution continued to improve [26], thus enhancing the electrostatic adsorption capacity of the tested fiber for Cu^{2+} and Zn^{2+}. However, the ionic strength continued to increase (I = 0.1 mol/L), and Na^+ could have competitive adsorption on $Cu^{2+}$and Zn^{2+}. As a result, the adsorption of Cu^{2+} and

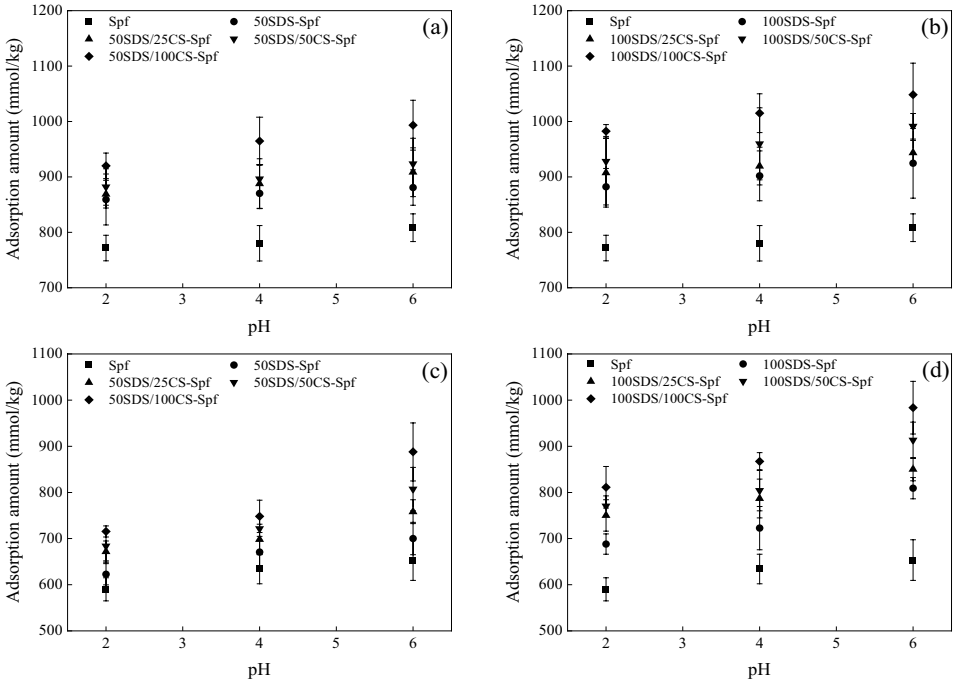

Fig. 4. Effect of pH on the adsorption of Cu^{2+} (a and b) and Zn^{2+} (c and d).

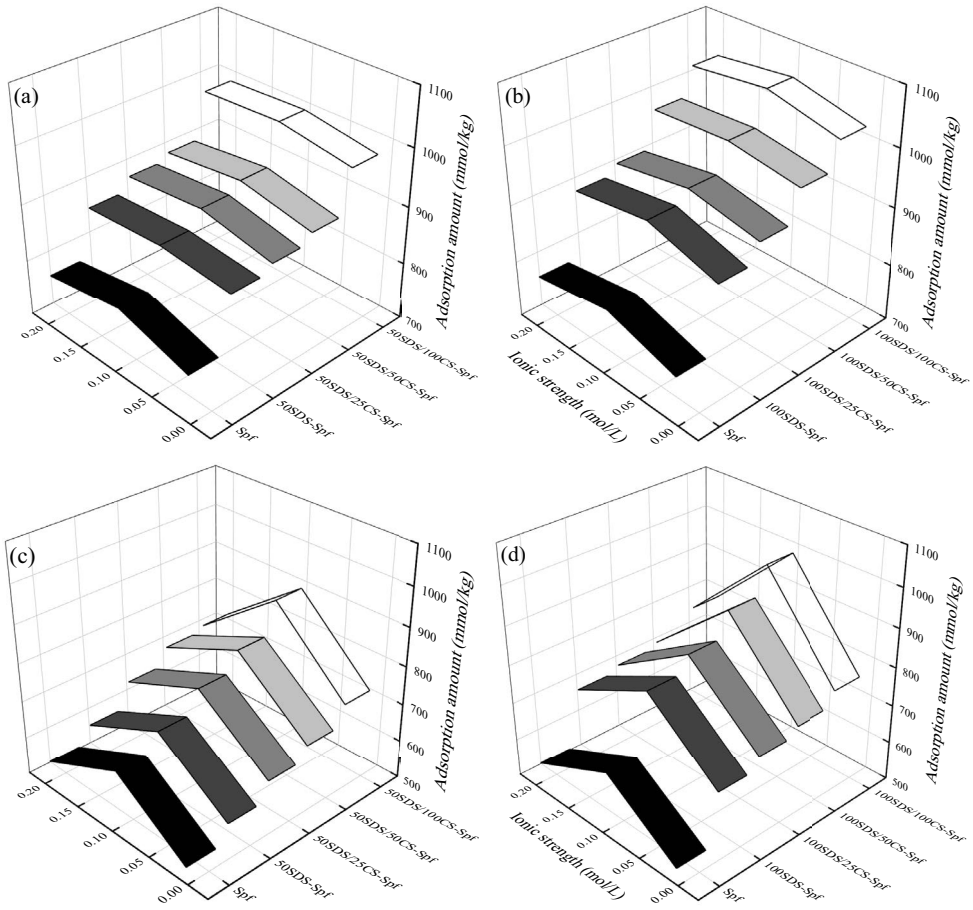

Fig. 5. Effect of ionic strength on Cu^{2+} and Zn^{2+} adsorption.

Zn^{2+} on the tested fiber weakened. Meanwhile, the increase in ionic strength led to the compression of the double electric layer on the fiber surface, the reduction in electrostatic attraction distance, and the mutual exclusion of the same ions, ultimately preventing Cu^{2+} and Zn^{2+} from approaching the negative charge point on the fiber surface [27].

3.5. Adsorption mechanism of Cu^{2+} and Zn^{2+} on the test materials

SDS has a hydrophobic carbon chain with a negatively charged sulfonic hydrophilic group at the end. The molecules of SDS are bonded with one another by hydrophobic carbon chains and extend outward [22]. When Spf was modified by SDS, it easily combined with the organic phase on the outer surface of Spf through the hydrophobic carbon chains, leaving the negative sulfonic group exposed to adsorb Cu^{2+} and Zn^{2+}. SDS-Spf had good ion-exchange capacity, and Cu^{2+} and Zn^{2+} adsorption occurred through ion exchange, which was a chemical endothermic reaction. SDS/CS-Spf can effectively change the surface and internal structure of Ap-C and obtain more active functional groups and adsorption sites [24]. The SDS/CS-Spf materials can react with Cu^{2+} and Zn^{2+} through electrostatic attraction, surface chelation, chemical precipitation, and ion exchange.

The basic physico-chemical properties of the tested materials in Table 1 and the adsorption parameters were linearly fitted, and the results are shown in Table 4. The pH of the materials was significantly negatively correlated with qm and b, whereas CEC and S_{BET} were highly positively correlated with q_m and b. These results showed that the pH, CEC, and S_{BET} of the materials were the key factors determining the adsorption amount of Cu and Zn^{2+}.

4. Conclusion

(1) The q_m of Cu^{2+} and Zn^{2+} on the tested samples maintained at 1,007.60–1,156.03 (Cu^{2+}) and 856.08–970.50 mmol/kg (Zn^{2+}), and showed a trend of SDS/CS-Spf > SDS-Spf > Spf.
(2) At 10°C–30°C, the adsorption amount of Cu^{2+} and Zn^{2+} on the tested materials increased with increasing temperature, and the adsorption exhibited a spontaneous, endothermic, and entropy-increasing process.
(3) High pH facilitated the adsorption of Cu^{2+} and Zn^{2+} on the tested materials in the pH range of 2–6. With the increase in ionic strength, the adsorption amount of Cu^{2+} and Zn^{2+} all increased first and then decreased, reaching the peak value at an ionic strength of 0.1 mol/L.
(4) The pH, CEC, and S_{BET} of the different SDS/CS-Spfs were the key factors determining the adsorption amount of Cu and Zn^{2+}.

Acknowledgements

The authors wish to acknowledge and thank the Sichuan Transportation Technology Project (2021-ZL-8), the Fundamental Research Funds of China West Normal University (20A022), the Tianfu Scholar Program of Sichuan Province (2020–17)

Conflict of interests

The authors declare that they have no conflict of interest.

References

[1] L. Shukla, N. Jain, A review on soil heavy metals contamination: effects, sources and remedies, Appl. Ecol. Environ. Sci., 10 (2022) 15–18.
[2] S.X. Fan, Z.T. Gan, M.J. Li, Z.Q. Zhang, Q. Zhou, Progress of assessment methods of heavy metal pollution in soil, Chin. Agric. Sci. Bull., 26 (2010) 310–315.
[3] M.F. Chen, Review on heavy metal remediation technology of soil and groundwater at industrially contaminated site in China, Bull. Chin. Acad. Sci., 29 (2014) 327–335.
[4] X. Tao, H. Yang, R. Ji, A.M. Li, Stabilizers and their applications in remediation of heavy metal-contaminated soil, Soils, 48 (2016) 1–11.
[5] L.Y. Hou, X.B. Zeng, Y.Z. Zhang, Application and outlook of alien earth soil-improving technology in arsenic-contaminated soil remediation, Chin. J. Eco-Agric., 23 (2015) 20–26.
[6] Y.H. Sun, F. Guan, X.L. Xu, Y.Q. Lin, Study of the effects of column leaching on remediation of chromium contaminated soils, Environ. Prot. Sci., 42 (2016) 113–118.
[7] Y.M. Zhu, D.Z. Wei, Biosorption of Mycobacterium phlei to the heavy metal ions Pb^{2+}, Zn^{2+}, Ni^{2+} and Cu^{2+}, J. Northeast Univ. (Nat. Sci.), 24 (2003) 91–93.
[8] J.H. Yuan, R.K. Xu, Progress of the research on the properties of biochars and their influence on soil environmental functions, J. Ecol. Environ., 20 (2011) 779–785.
[9] J.J. Liu, X. Yang, K.P. Lu, X.K. Zhang, H.G. Huang, H.L. Wang, Effect of bamboo and rice straw biochars on the transformation and bioavailability of heavy metals in soil, Acta Sci. Circumst., 35 (2015) 3679–3687.
[10] H.Y. Deng, J.C. Jiang, W.B. Li, X.Y. Chen, Y.Z. Zeng, T. Li, Study on adsorption characteristics of Cu^{2+} by bacteria-biochar-magnetized biochar composites, Environ. Sci. Technol., 42 (2019) 101–107.
[11] Z.M. Chen, Y. Fang, Y.L. Xu, The adsorption effect and influencing factors of rice straw biochar on heavy metal Pb^{2+}, Acta Sci. Circumst., 32 (2012) 769–776.
[12] J. Zhu, P. Wang, K.L. Li, M.J. Lei, W.L. Luo, Fixation effects and mechanisms of diatomite on pb in contaminated soil, Chin. Agric. Sin. Bull., 28 (2012) 240–245.
[13] Y.F. Wang, M. Li, W.B. Li, Y.T. Jia, M.Q. Liu, Y.Y. Song, Adsorption effect of Cr(VI) by purple soil amended with bacterial powder and biomass, Environ. Sci. Technol., 45 (2022) 44–50.
[14] L. Yang, B. Li, C.Q. Wang, Q.C. Liu, Q.P. Zhang, R. Xiao, Y.D. Li, Effect of modified biochars on soil cadmium stabilization in paddy soil suffered from original or exogenous contamination, Chin. J. Environ. Sci., 37 (2016) 3562–3574.
[15] L.K. Zhang, Y. Wang, W.D. Wang, Y.M. Li, P. Sun, J.H. Han, Q.H. Jiang, The preparation of biochar-supported nano-hydroxyapatite and its adsorption of Pb^{2+}, Chem. Ind. Eng. Prog., 37 (2018) 3492–3501.
[16] W.B. Li, Z.F. Meng, Z. Liu, Q. Wu, S.E. Xu, J. Zhu, Enhanced absorption of Cr(VI) on Lou soil by amphoteric and amphoteric cationic modified bentonite, Acta. Sci. Circumst., 36 (2016) 3810–3817.
[17] J.X. Yu, R.A. Chi, Y.L. Xu, Y.F. Zhang, Preparation of modified sugarcane bagasse and its comprehensive chemical experiment of adsorption performance toward heavy metal ions, Exp. Technol. Manage., 32 (2015) 39–42.
[18] W.B. Li, J. Xie, Y.F. Zhang, L. Zhu, H.Y. Deng, L. Kang, T. Li, Z.F. Meng, Adsorption characteristics of Cu^{2+} on different saponified pericarps, Ion Exch. Adsorpt., 36 (2020) 325–334.
[19] J. Xie, H.Y. Deng, L. Zhu, Y.F. Zhang, W.B. Li, D. Wang, Z.F. Meng, Preparation of amphoteric modified magnetized carbon and its adsorption to Cu(II), Desal. Water Treat., 194 (2020) 180–186.

[20] T. Xie, W.B. Li, Z.F. Meng, H.Y. Lu, S. Ren, Y. Sambath, Studies on Cr(VI) and Cd^{2+} adsorption onto bentonite modified by a BS-12+DTAB complex, J. Agro-Environ. Sci., 36 (2017) 1778–1786.
[21] W.B. Li, Z. Liu, Z.F. Meng, S. Ren, S.E. Xu, Y. Zhang, M.Y. Wang, Composite modification mechanism of cationic modifier to amphoteric modified kaolin and its effects on surface characteristics, Int. J. Environ. Sci. Technol., 13 (2016) 2639–2648.
[22] J.T. Wang, Z.F. Meng, Y.T. Yang, S.Y. Yang, B. Li, L.L. Ma, S.E. Xu, Effect of SDS on the adsorption of Cd^{2+} onto amphoteric modified bentonites, Environ. Sci., 35 (2014) 2596–2603.
[23] M. Yang, J.F. Ke, X.M. He, N.N. Lei, Q.W. Zhang, Adsorption of Cu^{2+} in aqueous solution by sodium hydroxide modified zeolite, Environ. Pollut. Control., 39 (2017) 314–318.
[24] W. Liu, T.T. Wang, L. Huang, W.B. Li, X.Z. Ning, H.Y. Deng. Adsorption of Cu^{2+} and Cd^{2+} on sierozem compositely modified by zwitterionic and anionic modifier, Desal. Water Treat., 240 (2022) 237–246.
[25] H.Y. Deng, W.B. Li, Y. Zheng, X.H. Zhu, Y.Y. Tian, W.X. Yan, Z.F. Meng, G.C. Chen, Study on the enhanced adsorption of Cu^{2+} in different purple soil layers by amphoteric bentonite, Earth Environ., 46 (2018) 403–409.
[26] X.L. Li, W.B. Li, H.Y. Deng, T. Li, D. Wang, Enhanced adsorption of Cu^{2+} on purple soil by amphoteric-modified materials, Desal. Water Treat., 196 (2020) 150–158.
[27] H.Y. Deng, X.L. Li, W.B. Li, L. Kang, X.H. Zhu, Z.F. Meng, H. Gao. Effect of different amendment materials on adsorption of Cu^{2+} in purple soil, Earth Environ., 47 (2019) 81–87.